Magn Reson Med Sci, Vol. 13, No. 4, pp. 239–249, 2014 doi:10.2463/mrms.2013-0117


**MAJOR PAPER**

# Operator-bias-free Comparison of Quantitative Perfusion Maps Acquired with Pulsed-continuous Arterial Spin Labeling and Single-photon-emission Computed Tomography

Takashi Iwanaga[1], Masafumi Harada[2*], Hitoshi Kubo[2†], Yasuhiro Funakoshi[1], Yamato Kunikane[3], and Tsuyoshi Matsuda[4]

[1]*Department of Medical Imaging, Institute of Health Biosciences, The University of Tokushima Graduate School 3–18–15 Kuramoto-cho, Tokushima 770–8503, Japan*
[2]*Department of Radiology, Institute of Health Biosciences, The University of Tokushima Graduate School*
[3]*Department of Radiology, Tokushima University Hospital*
[4]*GE Healthcare Japan Corporation, Ltd.*

(Received November 25, 2013; Accepted April 2, 2014; published online August 27, 2014)

Purpose: We compared the regional cerebral blood flow (rCBF) obtained by pulsed continuous arterial spin labeling (pCASL) and iodine-123-N-isopropyl-p-iodoamphetamine (IMP) single photon emission computed tomography (SPECT) using 3-dimensional stereotactic region-of-interest (ROI) software for automated definition of ROIs in anatomic regions of the brain.

Methods: Thirteen patients with cerebrovascular occlusive disease and three with transient ischemic attacks underwent pCASL and IMP SPECT imaging. We compared rCBF values of each anatomic region and calculated the correlation coefficients between pCASL and IMP SPECT. We also calculated the asymmetry index (AI) using ROIs in contralateral regions of the hemispheres.

Results: The rCBF values calculated from pCASL and IMP SPECT were comparable in most segments, but rCBF in the thalamus ($P < 0.0001$) and hippocampus ($P = 0.0006$) was significantly higher measured by pCASL than IMP SPECT. The correlation of rCBF between pCASL and IMP SPECT in the affected hemisphere ($r = 0.50$) tended to be lower than that in the normal hemisphere ($r = 0.59$), but not significantly different ($P = 0.25$). Moreover, there was a fixed bias for underestimation of rCBF by pCASL ($P = 0.0047$) in the affected hemisphere. The calculated AI showed a significant relationship between methods ($r = 0.79$, $P < 0.0001$).

Conclusion: The rCBF obtained by pCASL had positive relationships with IMP SPECT. However, it should be considered that pCASL tends to have a weak relationship with IMP SPECT in some normal regions and regions affected by cerebrovascular occlusive disease.

**Keywords:** ***arterial spin labeling*, *iodine-123-N-isopropyl-p-iodoamphetamine*, *pulsed continuous arterial spin labeling*, *regional cerebral blood flow*, *3-dimensional stereotactic region-of-interest software***

## Introduction

Arterial spin labeling (ASL) is a magnetic resonance (MR) imaging technique performed without injection of contrast medium to assess perfusion in tissue.[1–3] In this technique derived from the use of an endogenous tracer, labeling of the magnetization of water molecules in arterial blood by saturation or inversion pulses produces a change in the nuclear MR signal as arterial blood perfuses into tissue. This technique has several advantages for measur-

*Corresponding author, Phone: +81-88-633-9283, Fax: +81-88-633-7174, E-mail: masafumi@tokushima-u.ac.jp
†Present affiliation, Advanced Clinical Research Center, Fukushima Medical University

ing cerebral blood flow (CBF) in the clinical setting; it is noninvasive and repeatable and does not require use of an exogenous medium. These advantages are especially useful for pediatric patients, patients with allergies, and patients with renal dysfunction at risk for developing nephrogenic systemic fibrosis (NSF).[4]

ASL perfusion quantification relies on the change in signal between labeled images, in which magnetization of the arterial blood is inverted or saturated, and control images, in which the magnetization is fully relaxed. Typically, ASL is a technique with very low signal-to-noise ratio (SNR) because of both the limits of the $T_1$ relaxation time of arterial blood and the transit time from the labeling plane to the imaging plane. Consequently, the change in perfusion signal by ASL between the control and labeled images accounts for only one to 2% of signal. The 2 major ASL methods are continuous (CASL) and pulsed (PASL). CASL uses a constant gradient and a radiofrequency (RF) pulse to create a condition of adiabatic inversion driven by blood flow,[1,2] and PASL uses an instantaneous RF pulse to invert a slab of arterial blood.[3] Wang and associates reported that the raw signal measured with CASL is approximately 25% greater than that with PASL,[5] but labeling efficacy is slightly lower with CASL.[1,6,7] Furthermore, it is known that transit time effects affect CASL less than PASL, which causes systematic errors in quantitative CBF measurements in ASL.[8,9]

Recent technical advances have resulted in the development of pseudo- or pulsed continuous ASL (pCASL), an intermediate method that employs a train of discrete RF pulses to mimic flow-driven adiabatic inversion to take advantage of the superior SNR of CASL and the greater tagging efficiency of PASL.[10,11] In addition, the high magnetic field strength is expected to improve SNR by taking advantage of the increased $T_1$ relaxation time of arterial blood. Good agreements have already been found between CBF obtained by pCASL at 3.0 tesla and other modalities, such as positron emission tomography (PET) and dynamic susceptibility contrast (DSC) MR imaging.[12,13]

Iodine-123-N-isopropyl-p-iodoamphetamine (IMP) single photon emission computed tomography (SPECT) using autoradiography (ARG) is an established standard method to assess CBF, with substantial evidence accumulated in nuclear medicine. It is known that CBF values show good correlation between IMP SPECT and PET using $H_2{}^{15}O$ or $C^{15}O_2$.[14,15]

In patients with acute ischemic disease, simple and expeditious assessment of CBF is required to help decide the optimal therapeutic approach, which may include noninvasive or invasive recanalization. ASL can be added to routine images of non-contrast MR imaging examination, and follow-up is easily repeatable, so it is desirable to determine whether this technique can be applied to assess the CBF of patients with cerebrovascular disease. At present, nuclear medicine studies are commonly used to assess CBF. The rCBF values obtained by ASL and nuclear medicine studies may differ because the signal sources differ. It may also be important to understand how the characteristics of rCBF values calculated by ASL differ from those derived from nuclear medicine techniques. Good agreement has been reported between ASL and nuclear medicine studies.[12,16–18] However, these studies have usually involved the manual setting of regions of interest (ROI) on the CBF map, introducing inter-rater variability and making detailed comparisons of brain regions difficult.

We compared the quantitative rCBF obtained by pCASL and IMP SPECT in patients with cerebrovascular occlusive disease and used automatic ROI-setting software free of operator bias to compare detailed anatomic regions of the brain.

## Materials and Methods

*Subjects and instruments*

Subjects were 15 patients (10 men, 5 women; mean age, 69 years; range, 43 to 91 years) with suspected cerebrovascular occlusive disease. Two had middle cerebral artery (MCA) occlusion, one had both MCA and cervical internal carotid artery (ICA) stenosis, nine had cervical ICA occlusion or stenosis, and 3 patients transient ischemic attacks (TIA) (Table). The time from symptom onset to the patient's coming to the hospital varied considerably among patients. At the initial visit, the National Institutes of Health Stroke Scale (NIHSS) was assessed. Stroke was suspected on the basis of clinical signs, and MR imaging was given priority over CT. Ten patients proved to have acute ischemic attacks within 7 days of symptom onset. Two of these had chronic lacunar infarctions in the white matter, but MR imaging showed no major stroke. One of the ten (Subject 5) underwent intravenous thrombolytic treatment. Other patients diagnosed with stroke for whom thrombolytic treatment was counterindicated received conventional antiplatelet treatment.

Our hospital's institutional ethics committee approved the study, and after giving informed consent, all patients underwent both pCASL and IMP SPECT studies in addition to routine clinical examination. The intervals between the 2 studies were

**Table.** Clinical profile of all subjects

| Patient number | Age (years)/ Sex | Symptomatic state (NIHSS at first visit/42) | Delay of onset to time of examinations MR imaging/ SPECT | Etiology and diagnosis |
|---|---|---|---|---|
| 1 | 91/F | Right hemiparesis (4/42) | Day 1/ Day 2 | Left MCA occlusion/ Left WM (corona radiata) focal lacunar infarction |
| 2 | 63/M | Left hemiparesis (3/42) | Day 1/ Day 1 | Right MCA occlusion, Right cervical ICA severe stenosis (90%)/ Right MCA region multiple infarction (cortex of the insula, opercular part, caudate nucleus and MCA-PCA cortical watershed area) |
| 3 | 73/F | Left hemiparesis, dysarthria (6/42) | Day 4/ Day 4 | Right MCA occlusion/ Right nucleus basalis (caudate nucleus) infarction |
| 4 | 81/F | Left hand numbness (0/42) | Day 1/ Day 3 | Right cervical ICA severe stenosis (90%)/ Right WM (anterior limb of internal capsule) focal lacunar infarction |
| 5 | 84/M | Aphasic deficit (7/42) | Day 1/ Day 1 | Left cervical ICA occlusion/ Left WM (corona radiata) lacunar infarction |
| 6 | 82/M | Appearance of dysarthria (2/42) | Day 2/ Day 2 | Right cervical ICA severe stenosis (90%)/ Right MCA region multiple infarction (opercular part and MCA-PCA cortical watershed area) |
| 7 | 43/M | Consciousness disturbance (5/42) | Day 2/ Day 4 | Right cervical ICA occlusion/ Right MCA region multiple infarction (cortex of the insula, ACA-MCA and MCA-PCA cortical watershed area) |
| 8 | 61/M | Left hemiparesis (2/42) | Day 3/ Day 3 | Right cervical ICA occlusion/ No apparent infarcts |
| 9 | 69/M | Right upper limb numbness (2/42) | Day 9/ Day 5 | Left cervical ICA severe stenosis (90%)/ Left WM (corona radiata) and MCA-PCA cortical watershed area infarction |
| 10 | 60/M | Left hemiparesis (7/2) | Day 24/ Day 15 | Right cervical ICA occlusion/ Right WM (posterior limb of internal capsule) chronic lacunar infarction |
| 11 | 73/M | Dysarthria (0/42) | Day 34/ Day 33 | Left cervical ICA occlusion/ Left WM (corona radiata) chronic lacunar infarction |
| 12 | 75/M | Dizziness attacks (0/42) | 2 months/ 2 months | Left cervical ICA mild stenosis (40%)/ Left WM (corona radiata) chronic lacunar infarction |
| 13 | 53/F | Right upper limb numbness (0/42) | Day 1/ Day 1 | TIA/ No apparent infarcts |
| 14 | 69/F | Left upper limb numbness, dysarthria (0/42) | Day 1/ Day 2 | TIA/ No apparent infarcts |
| 15 | 61/M | Left upper limb cataplexy (0/42) | Day 26/ Day 21 | TIA/ No apparent infarcts |

ACA, anterior cerebral artery; F, female; ICA, internal carotid artery; M, male; MCA, middle cerebral artery; MR, magnetic resonance; NIHSS, National Institutes of Health Stroke Scale; PCA, posterior cerebral artery; SPECT, single photon emission computed tomography; TIA, transient ischemic attack; WM, white matter

0 to 9 days (mean 1.87 days) to ensure no thrombolytic therapy was performed during pCASL and IMP SPECT imaging. Subject 5 underwent both examinations for comparison after thrombolytic treatment.

*pCASL*

MR imaging was performed using a 3.0-T whole-body scanner (Signa Excite HDx, GE Healthcare, Waukesha, WI, USA) with an 8-channel phased-array coil. PCASL was added to conventional non-contrast MR imaging examinations. Conventional MR imaging sequences included diffusion-weighted imaging (DWI), $T_2$*-weighted imaging, 3-dimensional (3D) time-of-flight MR angiography (MRA), and $T_2$ fluid attenuated inversion recovery (FLAIR).

We developed the pCASL sequence according to the report of Dai and colleagues.[11] The sequence consisted of pulsed continuous labeling, background suppression, 3D fast-spin-echo acquisition with an interleaved stack spiral readout, and centric ordering in the slice encoding direction. Measurement conditions were: repetition time (TR), 4632 ms; echo time (TE), 10.5 ms; labeling duration, 1500 ms; post-labeling delay, 1500 ms; field of view (FOV), 24 cm; 512 sampling points on 8 arms; reconstructed matrix, 128 × 128; slice thickness, 5 mm; slice number, 32; number of excitations (NEX), 2; and total scan time, 3 min 15 s. In the same sequence, proton density images required for CBF quantification were made. The following formulas were applied to calculate quantitative rCBF from pCASL images in each patient in accordance with the description of Alsop and Detre.[8]

$$f = \frac{\lambda\left(1-\exp\left(-\frac{t_{sat}}{T_{1g}}\right)\right)\exp\left(\frac{w}{T_{1b}}\right)}{2\alpha T_{1b}\left(1-\exp\left(-\frac{t_l}{T_{1b}}\right)\right)}\frac{(S_c-S_l)}{S_{PDref}},$$

where $f$ = rCBF [mL/100 g/min], and $S_c$ is the signal intensity in the control images and $S_l$ is that in the labeled images. $S_{PDref}$ is the proton density image intensity; $T_{1b}$, the $T_1$ of blood (1600 ms); $T_{1g}$, the $T_1$ of gray matter (1200 ms); $t_{sat}$, a saturation time of 2000 ms in the flow-attenuated proton density image; $\alpha$, the labeling efficiency, assumed to be 95% for labeling multiplied by 75% for background suppression; $\lambda$, the brain-blood partition coefficient 0.9; $t_l$, the labeling duration (1500 ms), and $w$, the post-labeling delay time (1500 ms). The post-labeling delay time was introduced to reduce the influence of the transit time effect and vascular artifacts, which causes under- or overestimation of the rCBF.[8,19–21]

*SPECT*

In the SPECT study, we used a 2-detector apparatus (E.CAM dual-head gamma camera, Toshiba Medical Systems Corp., Tokyo, Japan) with fan beam collimators and injected IMP as a radioisotope tracer for cerebral perfusion. SPECT images were acquired in a 64 × 64 matrix by continuous rotation for 28 min (7 rotations, 4 min/rotation) after injection of IMP (111 MBq). We applied comparatively long scan time and a 64 × 64 acquisition matrix to obtain enough radiation counts. Images were reconstructed by the ordered-subset expectation maximization method (OSEM) algorithm. The μ-map obtained from projection data was used for both attenuation correction and scatter correction when transmission-dependent convolution subtraction (TDCS) was applied. One-point arterial blood sampling from the brachial artery was performed 10 min after IMP administration to quantify cerebral blood flow using the ARG method.[14,15,22]

*Three-dimensional stereotactic region-of-interest template*

The 3D stereotactic ROI template (3DSRT; Fujifilm RI Pharma, Tokyo, Japan) is automated ROI analysis software deforms a normal brain template and establishes identical ROIs on anatomically standardized brain images to estimate rCBF objectively and reproducibly.[23] The 3DSRT template uses the algorithm of statistical parametric mapping (SPM99) software (Wellcome Department of Cognitive Neurology, Institute of Neurology, London, UK) to standardize anatomical coordinates based on those of the Montreal Neurological Institute (MNI). The final matched spatial resolution of pCASL and IMP SPECT images was 2.0 × 2.0 × 2.0 $mm^3$ (FOV, 158 × 190 mm; re-gridding matrix, 79 × 95). The ROI of 3DSRT was categorized into 12 segments–callosomarginal, precentral, central, parietal, angular, temporal, posterior cerebral, pericallosal, lenticular nucleus, thalamus, hippocampus, and cerebellum (Fig. 1). In all patients, we visually verified the accuracy of segmentation by 3DSRT and found good agreement for each anatomical region.

*Quantitative comparisons*

For quantitative comparisons, we used 11 of the 12 segments of the brain on the gray matter with 3DSRT, excluding that in the cerebellum because of the risk of crossed cerebellar diaschisis in patients with cerebrovascular occlusive disease. Additionally, findings in 3 of the 15 patients (Subjects

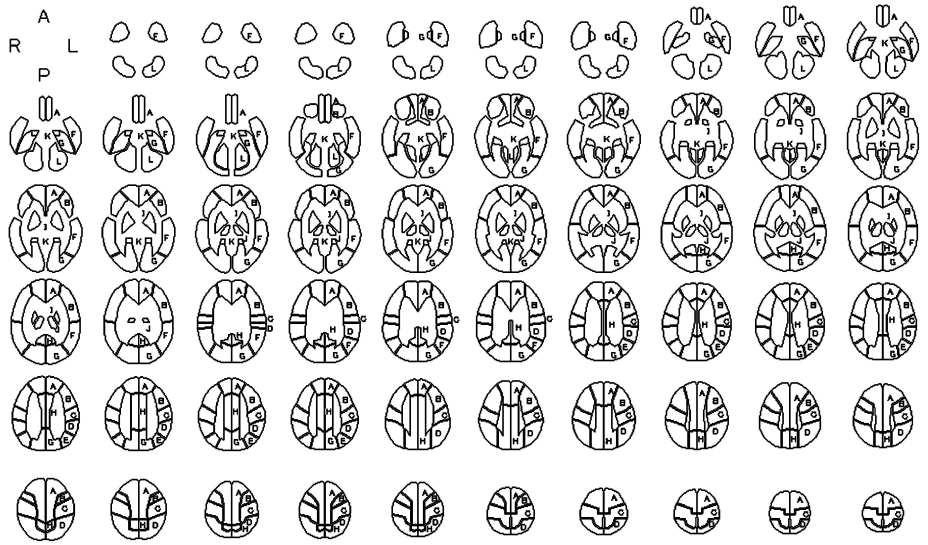

**Fig. 1.** The 12 segmental regions of interest (ROIs) in each hemisphere of the brain of the 3-dimensional (3D) stereotactic ROI template (SRT). A, callosomarginal; B, precentral; C, central; D, parietal; E, angular; F, temporal; G, posterior cerebral; H, pericallosal; I, lenticular nucleus; J, thalamus; K, hippocampus; and L, cerebellum.

13–15) were normal, and we categorized both hemispheres as normal. Therefore, we used 198 segments in 18 normal hemispheres and 132 segments in 12 affected hemispheres.

To compare rCBF obtained by pCASL and IMP SPECT, we compared the quantitative rCBF value of each of the 11 segments in the normal hemisphere between pCASL and IMP SPECT, calculated the correlation coefficient between pCASL and IMP SPECT from rCBF values in the normal hemisphere and the affected hemisphere, and calculated the asymmetry index (AI) of each segment for both pCASL and IMP SPECT according to the formula: $100 \times \{(\text{left} - \text{right})/(\text{left} + \text{right})\}$. Positive values indicated right-sided hypoperfusion, and negative values indicated left-sided hypoperfusion.

We used paired t test to compare rCBF and Pearson's correlation coefficient test to assess correlation coefficients. Bland-Altman plots were generated to display the spread of data and limits of agreement. The data were analyzed by using SPSS software (Ver. 12; SPSS Inc. Chicago, IL, USA). $P < 0.01$ was considered significant.

## Results

Figure 2 shows representative images of pCASL and IMP SPECT. Both show hypointensity in the right hemisphere, the affected side (Subject 2). Although the maximum intensity projection (MIP) image of MRA showed occlusion of the right middle cerebral artery (MCA), digital subtraction angiography revealed a collateral pathway via a leptomeningeal anastomosis (LMA) from the ipsilateral posterior cerebral artery (PCA). This patient had multiple localized infarctions in the region of the right MCA (Table). Although both CBF images showed hypoperfusion not only at the regions of infarction but also at the right thalamus outside the region of infarction, which was probably caused by diaschisis, scatter plots indicated a linear correlation between rCBF values obtained by pCASL and IMP SPECT.

Figure 3 shows the calculated quantitative rCBF value of each of the 11 segments of the normal hemisphere. The rCBF values in most segments indicated comparable values for pCASL and IMP SPECT. However, rCBF values in the thalamus ($P < 0.0001$) and hippocampus ($P = 0.0006$) segments were significantly higher obtained by pCASL than IMP SPECT.

Figure 4 shows scatter plots of the rCBF values in the normal and affected hemispheres. Significant linear correlations were found in both ($P < 0.0001$). The correlation coefficient tended to be lower of the affected hemisphere ($r = 0.50$) than the normal hemisphere ($r = 0.59$), but there was no significant difference ($P = 0.25$). In the normal hemisphere, a Bland-Altman plot demonstrated a mean difference in rCBF of $-1.10\,\text{mL}/100\,\text{g}/\text{min}$ between pCASL and IMP SPECT (Fig. 5a). There was no fixed ($P = 0.098$) or proportional bias ($r = 0.017$, $P = 0.831$). Therefore, there was good agreement between pCASL and IMP in the normal hemisphere.

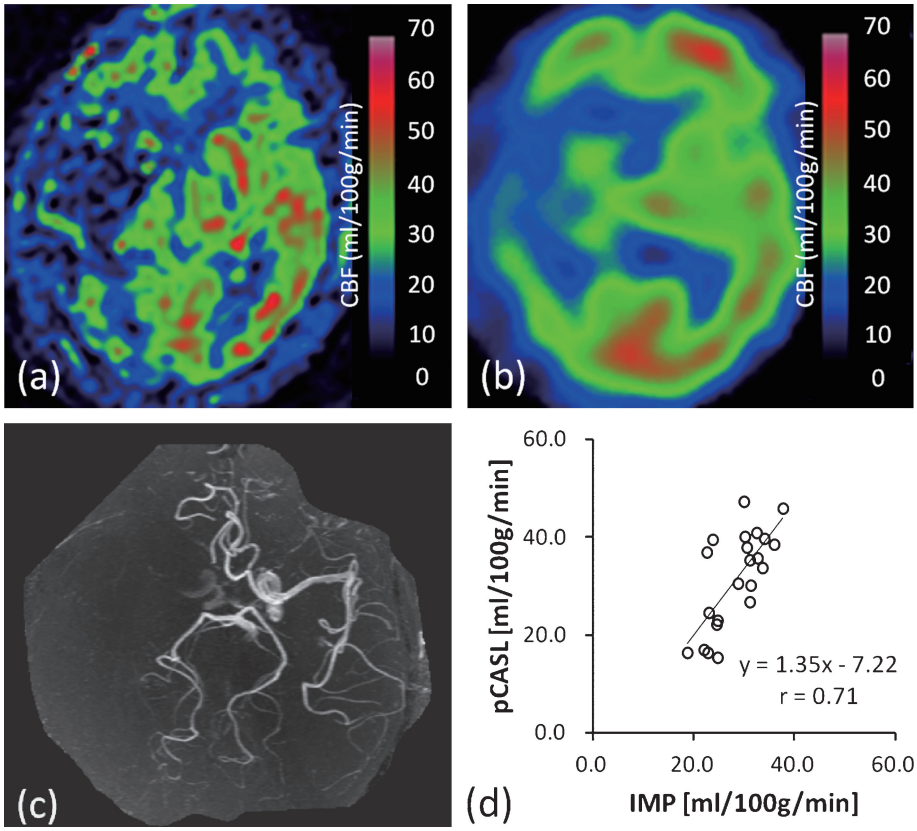


**Fig. 2.** A representative image of a 63-year-old man with multiple infarctions in the region of the right middle cerebral artery (MCA) (Subject 2). The images of cerebral blood flow (CBF) show hypointensity in the right hemisphere in both pulsed continuous arterial spin labeling (pCASL) (**a**) and iodine-123-N-isopropyl-p-iodoamphetamine (IMP) single photon emission computed tomography (SPECT) (**b**). The maximum intensity projection image of magnetic resonance angiography (MRA) (**c**) shows occlusion of the right MCA. Scatter plots of the regional CBF indicate a linear correlation between pCASL and IMP SPECT (**d**).

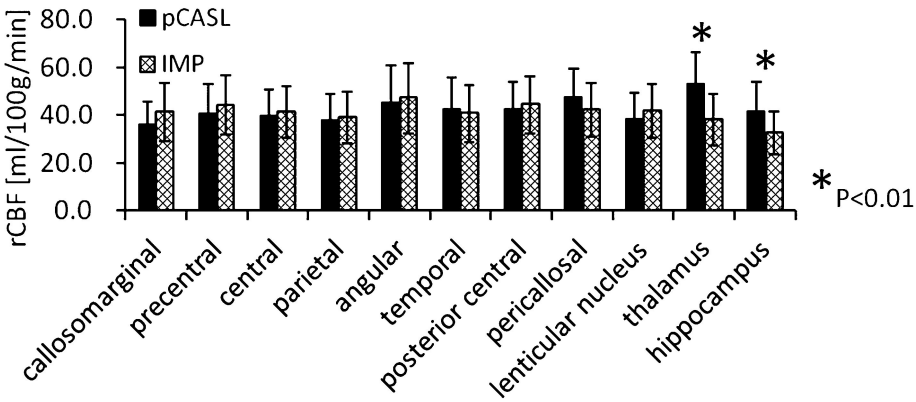


**Fig. 3.** The regional cerebral blood flow (rCBF) values of the 11 segments obtained by pulsed continuous arterial spin labeling (pCASL) and iodine-123-N-isopropyl-p-iodoamphetamine (IMP) single photon emission computed tomography (SPECT) of the mean overall normal hemispheres. The error bars indicate standard deviation. Significant differences between pCASL and IMP SPECT are found in 2 regions. PCASL rCBF values in the thalamus ($P < 0.0001$) and hippocampus ($P = 0.0006$) are significantly higher.

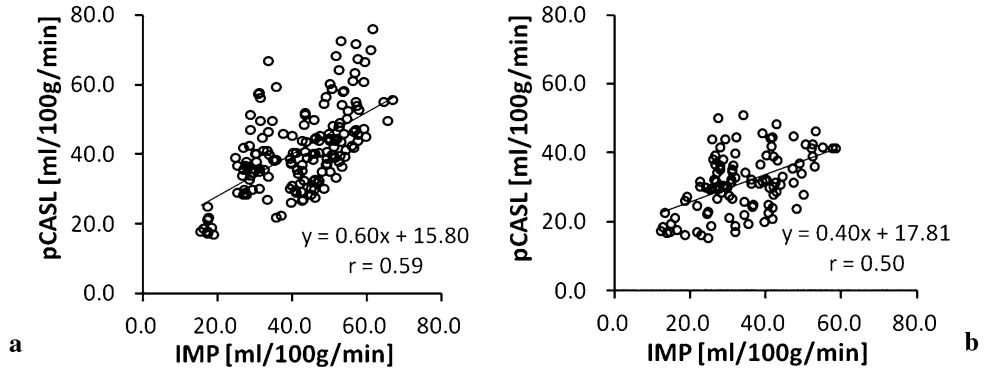


**Fig. 4.** Scatter plots of the values of regional cerebral blood flow (rCBF) in normal (**a**) and affected hemispheres (**b**) in 330 segments of 15 patients. Significant linear correlations are found in both ($P < 0.0001$). The correlation coefficient tends to be higher of the normal than affected hemisphere.

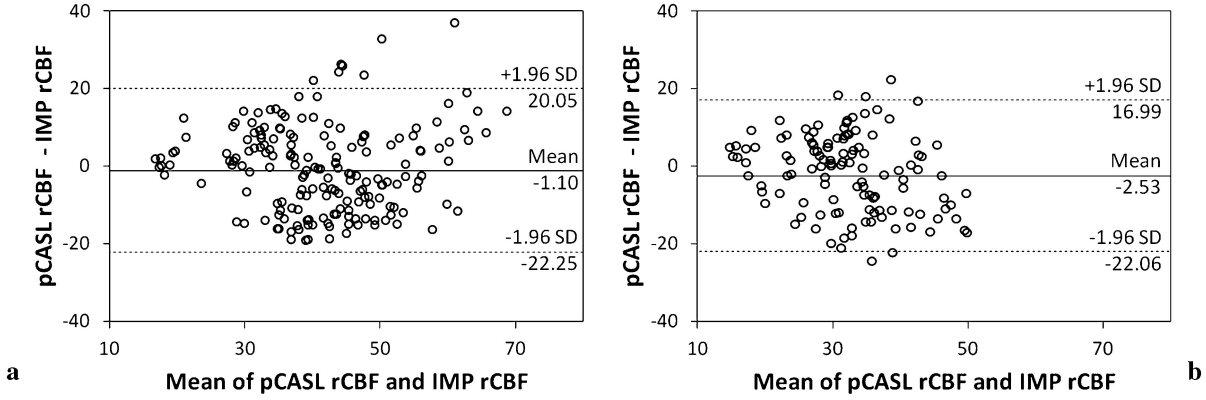


**Fig. 5.** Bland-Altman plot of the values of regional cerebral blood flow (rCBF) obtained by pulsed continuous arterial spin labeling (pCASL) and iodine-123-N-isopropyl-p-iodoamphetamine (IMP) single photon emission computed tomography (SPECT) in the normal (**a**) and affected hemispheres (**b**). The center line shows the mean of the difference, and the top and bottom dashed lines show $\pm 1.96 \times$ standard deviation (SD) of the differences.

On the other hand, in the affected hemisphere, a Bland-Altman plot demonstrated a mean difference in rCBF of $-2.53$ mL/100 g/min between pCASL and IMP (Fig. 5b). There was a fixed bias ($P = 0.0047$) of underestimation of rCBF by pCASL, but the bias of underestimation was approximately 10% of rCBF. There was no proportional bias ($r = -0.169$, $P = 0.052$).

Figure 6 shows the scatter plot of calculated AI. A significant linear relationship was found with a high correlation coefficient ($r = 0.79$, $P < 0.0001$), but AI values tended to be higher obtained with pCASL than IMP SPECT.

## Discussion

We compared pCASL and IMP SPECT in patients with cerebrovascular occlusive disease using 3DSRT software to avoid operator bias. Most studies comparing ASL and other brain perfusion methods have set ROIs manually on the CBF map,[12,16–18] but the manual setting of ROIs introduces inter-rater variability, which is avoided using 3DSRT because the software automatically draws the segmented ROI after registration to an anatomically standardized brain image. In our study, use of 3DSRT allowed detailed comparison in each region of the brain.

Several factors are known to cause errors in quantitative measurements of CBF with ASL, including transit time effects and vascular artifacts.[8,19,20] Transit time effects may cause underestimation of rCBF. Alsop's group suggested using post-labeling delay time (PLD),[8] the time between image acquisition and the labeling of arterial blood, to make the CASL sequence insensitive to transit time effects. If the PLD is shorter than the arrival time of labeled blood for the intended tissue, rCBF values lead to underestimation because we cannot differentiate the signals of control and labeled im-

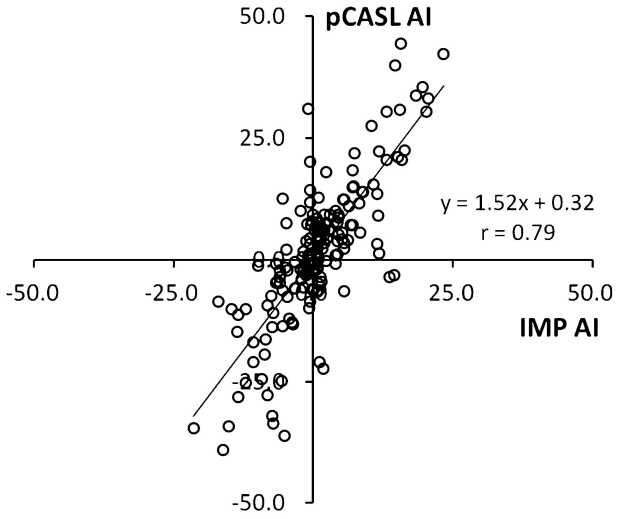


**Fig. 6.** Scatter plots of the calculated asymmetry index (AI). A significant linear relationship is found with a high correlation coefficient ($r = 0.79$, $P < 0.0001$). The AI values tend to be higher for pulsed continuous arterial spin labeling (pCASL) than iodine-123-N-isopropyl-p-iodoamphetamine (IMP) single photon emission computed tomography (SPECT).

ages. Therefore, the PLD must be longer than the arterial transit time for the intended tissues. However, increasing the PLD reduces the difference between signals of control and labeled images, which decay exponentially with the $T_1$ relaxation time in arterial blood. Vascular artifacts are observed at the time of image acquisition, and some labeled blood may be present in the arteries or arterioles rather than in the intended tissues. Such vascular artifacts will lead to overestimation of the rCBF.[19,20] Ye and associates[21] suggested using the crusher gradients and PLD to suppress the development of vascular artifacts in PASL. However, we performed pCASL without using crusher gradients because it is difficult to determine the adequate strength of bipolar gradients. This could account for the remaining vascular artifacts. We only introduced PLD to reduce the influence of transit time effects and vascular artifacts.

Our results showed comparable quantitative rCBF values between pCASL and IMP SPECT in most regions, except in the thalamus and hippocampus. The overestimation by CBF with ASL in gray matter is consistent with findings in earlier studies comparing ASL with image acquisition using a single PLD to PET,[16,24] and those studies attribute the overestimation mainly to the intravascular signal of microvessels, even when longer PLD times are used. The blood vessels feeding the thalamus are penetrating branches of the posterior communicating artery, anterior choroidal artery, and perforating branch of the posterior cerebral artery (PCA). Those of the hippocampus are the posterior communicating artery, anterior choroidal artery, and cortical branch of the PCA. Labeled blood remaining in these small feeding arteries can lead to overestimation of CBF.[21] Furthermore, rCBF can still be underestimated in hyperperfused regions with IMP SPECT because of lower imaging resolutions.[15] The thalamus and hippocampus are localized to a small region and hemmed in by white matter. Inclusion in the ROI of white matter signal with lower rCBF might yield partial volume effects.

Siewert and associates[25] reported slower flow in the posterior circulation than in the anterior and middle. Using echo-planar imaging with signal targeting and alternating radiofrequency (EPISTAR), as an example of a PASL technique, with a PLD of 1400 ms, they observed vascular artifacts in the cerebral cortex in the territory of the PCA and overestimated the rCBF. Therefore, they noted that a longer PLD (>2400 ms) might be necessary to image the posterior circulation. In our study, the rCBF in the territory of the PCA was not overestimated using pCASL with a PLD of 1500 ms. One reason is that PASL uses an instantaneous radiofrequency pulse to invert a slab of arterial blood, whereas pCASL uses a train of discrete RF pulses. In our study, the labeling duration in pCASL was 1500 ms, and the time from beginning of labeling to image acquisition was over 3000 ms.

In comparing correlation coefficients, we observed significant linear correlation between the rCBF of pCASL and IMP SPECT. However, the correlation coefficient of the affected hemisphere tended to be lower than that of the normal hemisphere. This difference may be influenced by transit time effects and vascular artifacts in pCASL. The hemisphere with arterial occlusion exhibits slow flow. In previous studies, patients with cerebrovascular disease and consequent prolonged arterial transit time required a PLD of at least 1500 ms in CASL[26] and at least 2400 ms in PASL.[25]

Subject 8 demonstrated obvious mismatch between pCASL and IMP SPECT in the affected hemisphere. pCASL showed delayed bright intravascular signal in the territory of the right MCA and focal low signal because the labeled arterial blood had not arrived in the watershed area of the right MCA to the PCA. In contrast, the IMP SPECT study showed normal perfusion (Fig. 7). In this case, arterial transit time was prolonged because of the cross-filling of the right anterior cerebral artery (ACA) and MCA from the left ICA circulation and the collateral pathway via the LMA from the left PCA (Fig. 7c). Therefore, pCASL showed sig-

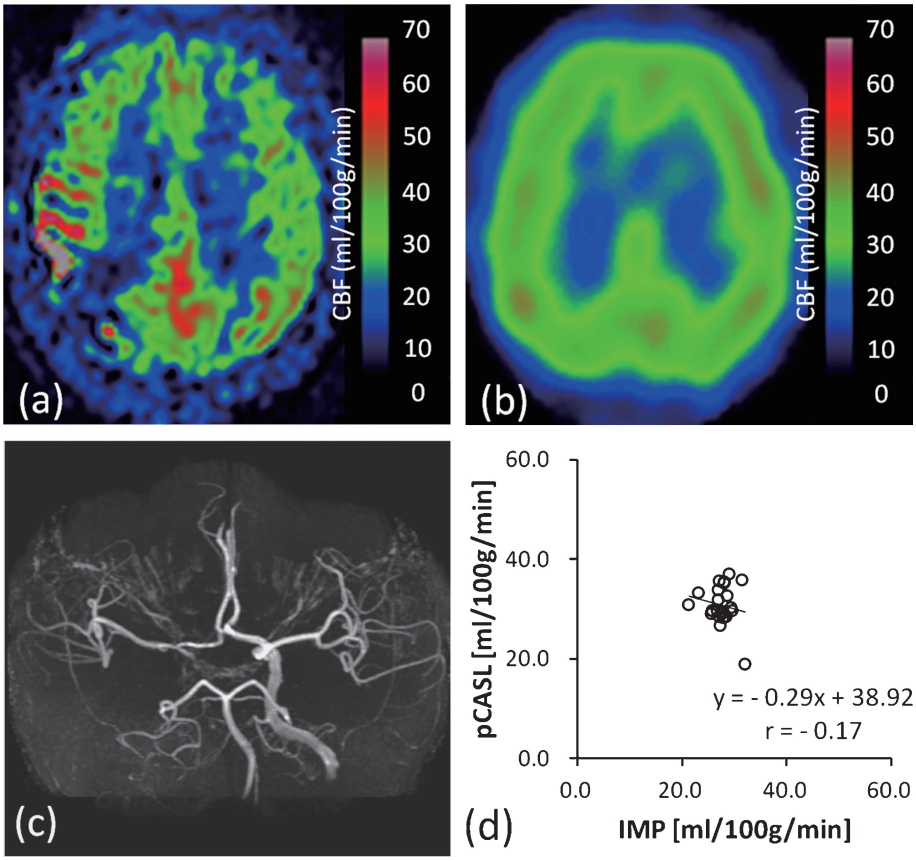


**Fig. 7.** Images of cerebral blood flow (CBF) show obvious mismatch between pulsed continuous arterial spin labeling (pCASL) and iodine-123-N-isopropyl-p-iodoamphetamine (IMP) single photon emission computed tomography (SPECT) of a 61-year-old man with occlusion of the right internal carotid artery (ICA) with no apparent infarcts (Subject 8). The CBF image with pCASL demonstrates bright intravascular signal and focal low signal in the territory of the right middle cerebral artery (MCA) and watershed area of the right MCA to the posterior cerebral artery (PCA) (**a**), and IMP SPECT shows normal perfusion (**b**). The maximum intensity projection image of magnetic resonance angiography (MRA) (**c**) shows occlusion of the right ICA with cross-filling of the right anterior artery (ACA) and MCA from the left ICA circulation. The scatter plots of regional CBF indicate a low correlation between pCASL and IMP SPECT (**d**).

nal variation in the affected hemisphere. ASL has also been reported to provide information regarding the presence of collateral cortical flow using both CASL and PASL.[25,27–30] The studies of the teams of Chalela, using CASL,[27] Viallon, using flow-sensitive alternating inversion recovery (FAIR) as an example of a PASL technique,[30] and Wang, using pCASL,[31] reported the cases of patients presenting with hyperperfusion in the ischemic territory. They explained hyperperfusion corresponding to bright intravascular signal with delayed arterial transit and luxury perfusion previously demonstrated by PET study.[32,33] The presence of hyperperfusion after stroke on ASL indicated reperfusion and collateralization, correlating with stroke severity and functional outcome. By contrast, Tanaka's team[34] reported longer $T_1$ values in the ischemic area and freer extavasation of water in the blood by disruption of the blood-brain barrier, which resulted in overestimation of CBF by ASL as hyperperfusion.

Regarding the bilateral difference in rCBF in pCASL and IMP SPECT, AI values were strongly related in both methods ($r = 0.79$, $P < 0.0001$). Therefore, we feel the quantitative rCBF values from pCASL as well as those calculated from IMP SPECT can be used to evaluate the site of ischemia. However, the AI values of pCASL tended to be higher than those of IMP SPECT, indicating that pCASL may overestimate the degree of ischemia. This is thought to result from a fixed bias of underestimation of rCBF by pCASL in the affected hemisphere (Fig. 5b).

Our study has several limitations. First, the time intervals from symptom onset to examination var-

ied, and the patient populations were inhomogeneous. However, we compared CBF maps obtained by pCASL and IMP SPECT studies as close as possible to one another. Moreover, we ensured there was no thrombolytic therapy during pCASL and IMP SPECT imaging. Second, though most of our patients had acute atherothrombotic infarction, fewer patients had acute embolic infarction of cerebral artery with rapid change in blood flow in a short time. Further studies are needed to establish the validity of pCASL in patients with acute embolic infarction. Third, with regard to the accuracy of segmentation using 3DSRT, previous studies estimated good correlation between 3DSRT and manual tracing methods in 10 (83.3%) of 12 brain segments, but poor correlation was seen in the pericallosal and hippocampal segments. Fourth, ROIs set automatically might include undesirable signals, such as from vascular artifacts and areas of focal signal loss because of transit time effects, and average such signals. This averaging effect would be unavoidable using 3DSRT. Finally, we compared IMP SPECT as a standard method. PET has become recognized as a standard for CBF quantification. There is a good correlation between CBF values obtained from IMP SPECT and PET, but it is known that the ARG method underestimates rCBF in areas of hyperperfusion and overestimates it in areas of hypoperfusion.[15] Nevertheless, IMP SPECT is an established standard method of CBF assessment and brings with it substantial clinical evidence of its utility.

In conclusion, without operator bias, we could calculate and compare rCBF values of pCASL and IMP SPECT in patients with cerebrovascular occlusive disease. Although pCASL correlates linearly with IMP SPECT, overestimation of the extent of ischemia by pCASL decreased the correlation of rCBF values by the 2 methods. The rCBF values in the thalamus and hippocampus would be higher by pCASL than IMP SPECT. It is important to recognize these different characteristics of pCASL perfusion imaging from those of conventional IMP SPECT when applying pCASL to patients with cerebrovascular ischemia.

## Acknowledgement

This study was supported by Grant-in-aid for Scientific Research (B) No. 21390346 from the Japan Society for the Promotion of Science (JSPS).

## References

1. Williams DS, Detre JA, Leigh JS, Koretsky AP. Magnetic resonance imaging of perfusion using spin inversion of arterial water. Proc Natl Acad Sci USA 1992; 89:212–216.
2. Detre JA, Leigh JS, Williams DS, Koretsky AP. Perfusion imaging. Magn Reson Med 1992; 23:37–45.
3. Wong EC, Buxton RB, Frank LR. Implementation of quantitative perfusion imaging techniques for functional brain mapping using pulsed arterial spin labeling. NMR Biomed 1997; 10:237–249.
4. Marckmann P, Skov L, Rossen K, et al. Nephrogenic systemic fibrosis: suspected causative role of gadodiamide used for contrast-enhanced magnetic resonance imaging. J Am Soc Nephrol 2006; 17:2359–2362.
5. Wang J, Alsop DC, Li L, et al. Comparison of quantitative perfusion imaging using arterial spin labeling at 1.5 and 4.0 Tesla. Magn Reson Med 2002; 48: 242–254.
6. Wong EC, Buxton RB, Frank LR. A theoretical and experimental comparison of continuous and pulsed arterial spin labeling techniques for quantitative perfusion imaging. Magn Reson Med 1998; 40:348–355.
7. Ye FQ, Smith AM, Yang Y, et al. Quantitation of regional cerebral blood flow increases during motor activation: a steady-state arterial spin tagging study. Neuroimage 1997; 6:104–112.
8. Alsop DC, Detre JA. Reduced transit-time sensitivity in noninvasive magnetic resonance imaging of human cerebral blood flow. J Cereb Blood Flow Metab 1996; 16:1236–1249.
9. Mildner T, Möller HE, Driesel W, Norris DG, Trampel R. Continuous arterial spin labeling at the human common carotid artery: the influence of transit times. NMR Biomed 2005; 18:19–23.
10. Wu WC, Fernández-Seara M, Detre JA, Wehrli FW, Wang J. A theoretical and experimental investigation of the tagging efficiency of pseudocontinuous arterial spin labeling. Magn Reson Med 2007; 58:1020–1027.
11. Dai W, Garcia D, de Bazelaire C, Alsop DC. Continuous flow-driven inversion for arterial spin labeling using pulsed radio frequency and gradient fields. Magn Reson Med 2008; 60:1488–1497.
12. Xu G, Rowley HA, Wu G, et al. Reliability and precision of pseudo-continuous arterial spin labeling perfusion MRI on 3.0T and comparison with (15)O-water PET in elderly subjects at risk for Alzheimer's disease. NMR Biomed 2010; 23:286–293.
13. Järnum H, Steffensen EG, Knutsson L, et al. Perfusion MRI of brain tumours: a comparative study of pseudo-continuous arterial spin labelling and dynamic susceptibility contrast imaging. Neuroradiology 2010; 52:307–317.
14. Iida H, Itoh H, Nakazawa M, et al. Quantitative mapping of regional cerebral blood flow using iodine-123-IMP and SPECT. J Nucl Med 1994; 35:2019–2030.
15. Iida H, Akutsu T, Endo K, et al. A multicenter val-

idation of regional cerebral blood flow quantitation using [123I]iodoamphetamine and single photon emission computed tomography. J Cereb Blood Flow Metab 1996; 16:781–793.
16. Kimura H, Kado H, Koshimoto Y, Tsuchida T, Yonekura Y, Itoh H. Multislice continuous arterial spin-labeled perfusion MRI in patients with chronic occlusive cerebrovascular disease: a correlative study with CO2 PET validation. J Magn Reson Imaging 2005; 22:189–198.
17. Arbab AS, Aoki S, Toyama K, et al. Brain perfusion measured by flow-sensitive alternating inversion recovery (FAIR) and dynamic susceptibility contrast-enhanced magnetic resonance imaging: comparison with nuclear medicine technique. Eur Radiol 2001; 11:635–641.
18. Arbab AS, Aoki S, Toyama K, et al. Optimal inversion time for acquiring flow-sensitive alternating inversion recovery images to quantify regional cerebral blood flow. Eur Radiol 2002; 12:2950–2956.
19. Roberts DA, Detre JA, Bolinger L, Insko EK, Leigh JS Jr. Quantitative magnetic resonance imaging of human brain perfusion at 1.5T using steady-state inversion of arterial water. Proc Natl Acad Sci USA 1994; 91:33–37.
20. Ye FQ, Pekar JJ, Jezzard P, Duyn J, Frank JA, McLaughlin AC. Perfusion imaging of the human brain at 1.5T using a single-shot EPI spin tagging approach. Magn Reson Med 1996; 36:217–224.
21. Ye FQ, Mattay VS, Jezzard P, Frank JA, Weinberger DR, McLaughlin AC. Correction for vascular artifacts in cerebral blood flow values measured by using arterial spin tagging techniques. Magn Reson Med 1997; 37:226–235.
22. Iida H, Itoh H, Bloomfield PM, et al. A method to quantitate cerebral blood flow using a rotating gamma camera and iodine-123 iodoamphetamine with one blood sampling. Eur J Nucl Med 1994; 21: 1072–1084.
23. Takeuchi R, Yonekura Y, Takeda SK, Fujita K, Konishi J. Fully automated quantification of regional cerebral blood flow with three-dimensional stereotaxic region of interest template: validation using magnetic resonance imaging—technical note. Neurol Med Chir (Tokyo) 2003; 43:153–162.
24. Ye FQ, Berman KF, Ellmore T, et al. H(2)(15)O PET validation of steady-state arterial spin tagging cerebral blood flow measurements in humans. Magn Reson Med 2000; 44:450–456.
25. Siewert B, Schlaug G, Edelman RR, Warach S. Comparison of EPISTAR and $T_2$*-weighted gadolinium-enhanced perfusion imaging in patients with acute cerebral ischemia. Neurology 1997; 48:673–679.
26. Detre JA, Alsop DC, Vives LR, Maccotta L, Teener JW, Raps EC. Noninvasive MRI evaluation of cerebral blood flow in cerebrovascular disease. Neurology 1998; 50:633–641.
27. Chalela JA, Alsop DC, Gonzalez-Atavales JB, Maldjian JA, Kasner SE, Detre JA. Magnetic resonance perfusion imaging in acute ischemic stroke using continuous arterial spin labeling. Stroke 2000; 31:680–687.
28. Lim CC, Petersen ET, Ng I, Hwang PY, Hui F, Golay X. MR regional perfusion imaging: visualizing functional collateral circulation. AJNR Am J Neuroradiol 2007; 28:447–448.
29. Altrichter S, Kulcsar Z, Jägersberg M, et al. Arterial spin labeling shows cortical collateral flow in the endovascular treatment of vasospasm after post-traumatic subarachnoid hemorrhage. J Neuroradiol 2009; 36:158–161.
30. Viallon M, Altrichter S, Pereira VM, et al. Combined use of pulsed arterial spin-labeling and susceptibility-weighted imaging in stroke at 3T. Eur Neurol 2010; 64:286–296.
31. Wang DJ, Alger JR, Qiao JX, et al. The value of arterial spin-labeled perfusion imaging in acute ischemic stroke: comparison with dynamic susceptibility contrast-enhanced MRI. Stroke 2012; 43: 1018–1024.
32. Marchal G, Young AR, Baron JC. Early postischemic hyperperfusion: pathophysiologic insights from positron emission tomography. J Cereb Blood Flow Metab 1999; 19:467–482.
33. Marchal G, Furlan M, Beaudouin V, et al. Early spontaneous hyperperfusion after stroke. A marker of favourable tissue outcome? Brain 1996; 119: 409–419.
34. Tanaka Y, Nagaoka T, Nair G, Ohno K, Duong TQ. Arterial spin labeling and dynamic susceptibility contrast CBF MRI in postischemic hyperperfusion, hypercapnia, and after mannitol injection. J Cereb Blood Flow Metab 2011; 31:1403–1411.
35. Nagasawa N, Yamakado K, Yamada T, et al. Three-dimensional stereotactic ROI template for measuring regional cerebral blood flow in 99mTc-ECD SPECT: comparison with the manual tracing method. Nucl Med Commun 2009; 30:155–159.